



Contents lists available at ScienceDirect

Journal of Traditional and Complementary Medicine

journal homepage: <http://www.elsevier.com/locate/jtcm>

Original Article

Dried mulberry fruit ameliorates cardiovascular and liver histopathological changes in high-fat diet-induced hyperlipidemic mice



Suriya Chaiwong^a, Usana Chatturong^a, Rachanee Chanasong^b, Watcharakorn Deetud^a, Kittiwot To-on^a, Supaporn Puntheeranurak^a, Ekarin Chulikorn^c, Tanwarat Kajsongkram^d, Veerada Raksanoh^a, Kroekkiat Chinda^a, Nanteetip Limpeanchob^e, Kanittaporn Trisat^e, Julintorn Somran^f, Nitra Nuengchamnon^g, Piya Prajumwong^a, Krongkarn Chootip^{a,*}

^a Department of Physiology, Faculty of Medical Science and Center of Excellence for Innovation in Chemistry, Naresuan University, Phitsanulok, Thailand

^b Department of Anatomy, Faculty of Medical Science, Naresuan University, Phitsanulok, Thailand

^c Department of Biochemistry, Faculty of Medical Science, Naresuan University, Phitsanulok, Thailand

^d Expert Center of Innovative Herbal Products, Thailand Institute of Scientific and Technological Research, Pathum Thani, Thailand

^e Department of Pharmacy Practice and Center of Excellence for Innovation in Chemistry, Pharmacological Research Unit, Faculty of Pharmaceutical Sciences, Naresuan University, Phitsanulok, Thailand

^f Department of Pathology, Faculty of Medicine, Naresuan University, Phitsanulok, Thailand

^g Science Laboratory Centre, Faculty of Science, Naresuan University, Phitsanulok, Thailand

ARTICLE INFO

Article history:

Received 4 August 2020

Received in revised form

7 February 2021

Accepted 8 February 2021

Available online 12 February 2021

Keywords:

Morus alba

Mulberry fruit

Hyperlipidemia

Cardiovascular

Liver

ABSTRACT

Background and aim: Metabolic disease encompasses most contemporary non-communicable diseases, especially cardiovascular and fatty liver disease. Mulberry fruits of *Morus alba* L. are a favoured food and a traditional medicine. While they are anti-atherosclerotic and reduce hyperlipidemic risk factors, studies need wider scope that include ameliorating cardiovascular and liver pathologies if they are to become clinically effective treatments. Therefore, the present study sought to show that freshly dried mulberry fruits (dMF) might counteract the metabolic/cardiovascular pathologies in mice made hyperlipidemic by high-fat diet (HF).

Experimental procedure: C57BL/6J mice were fed for 3 months with either: i) control diet, ii) HF, iii) HF+100 mg/kg dMF, or iv) HF+300 mg/kg dMF. Body weight gain, food intake, visceral fat accumulation, fasting blood glucose, plasma lipids, and aortic, heart, and liver histopathologies were evaluated. Adipocyte lipid accumulation, autophagy, and bile acid binding were also investigated.

Results and conclusion: HF increased food intake, body weight, visceral fat, plasma total cholesterol (TC) and low-density lipoprotein (LDL), TC/HDL ratio, blood glucose, aortic collagen, arterial and cardiac wall thickness, and liver lipid. Both dMF doses prevented hyperphagia, body weight gain, and visceral fat accumulation, lowered blood glucose, plasma TG and unfavourable TC/HDL and elevated plasma HDL beyond baseline. Arterial and cardiac wall hypertrophy, aortic collagen fibre accumulation and liver lipid deposition ameliorated in dMF-fed mice. Clinical trials on dMF are worthwhile but outcomes should be

Abbreviations: dMF, Dried mulberry fruit; DPPH, 2,2-diphenyl-1-picrylhydrazyl; HDL, high-density lipoprotein; LDL, low-density lipoprotein; TC, total cholesterol; TG, triglyceride.

* Corresponding author. Department of Physiology, Faculty of Medical Science, Naresuan University, Phitsanulok, 65000, Thailand.

E-mail addresses: krongkarn@gmail.com, krongkarn@nu.ac.th (K. Chootip).

Peer review under responsibility of The Center for Food and Biomolecules, National Taiwan University.

<https://doi.org/10.1016/j.jtcm.2021.02.006>

2225-4110/© 2021 Center for Food and Biomolecules, National Taiwan University. Production and hosting by Elsevier Taiwan LLC. This is an open access article under the CC BY-NC-ND license (<http://creativecommons.org/licenses/by-nc-nd/4.0/>).

holistic commensurate with the constellation of disease risks. Here, dMF should supplement the switch to nutrient-rich from current energy-dense diets that are progressively crippling national health systems. © 2021 Center for Food and Biomolecules, National Taiwan University. Production and hosting by Elsevier Taiwan LLC. This is an open access article under the CC BY-NC-ND license (<http://creativecommons.org/licenses/by-nc-nd/4.0/>).

1. Introduction

Life-style dominated by excess energy intake leads to wide range of disease processes collectively termed metabolic disease. These conditions are characterised by but not restricted to: hypertriglyceridemia, diabetes, hypercholesterolemia (especially very low- and low-density lipoprotein cholesterol (LDL)),^{1,2} hepatic steatosis^{3–5} and cardiovascular disease (atherosclerosis resulting in hypertension, myocardial infarction, and stroke).⁶ Vascular dysfunction is dominated by inflammation beginning with endothelial damage and discontinuity; loss of vasodilatory signalling; oxidised LDL entering the arterial intima, then engulfed by invading macrophages that become lipid-laden foam cells manifest as fatty streaks. Vascular smooth muscle cells proliferate and migrate: the arterial intima becomes fibrotic; platelets adhere to the damaged vascular wall thus triggering coagulation and compromised blood flow.^{7,8}

As fat accumulates, the adipocyte lipid capacity becomes limiting whereupon resident macrophages switch to inflammatory phenotypes, especially in visceral and perivascular adipose tissues.⁹ From the latter, inflammatory cytokines exacerbate vascular inflammation. Insulin and leptin resistance develops so excess circulating lipids are then removed by non-adipocyte lineages (ectopic fat: muscle, liver, etc.). However, the physiological mechanisms such as exercise or thermogenesis can no longer mobilise fat from refractory adipocytes and ectopic fat and fail to impact body weight. Autophagy recycles dysfunctional cell constituents but becomes less effective in metabolic syndrome¹⁰ and fatty liver disease.¹¹ The related lipophagy mobilises fats from cell lipid droplets from a variety of cells including hepatocytes. Lipophagy also may stimulate transdifferentiation of white adipocytes into brown fat cells, absent from obese patients, that metabolise lipids by uncoupled oxidative thermogenesis.¹²

Most current anti-atherogenic treatment strategies focus on antihypercholesterolemic treatments: (a) diets low in cholesterol or its precursor; (b) intestinal cholesterol absorption inhibitors, (c) PCSK9 inhibitors that remove LDL cholesterol, and (d) statins, the mainstay treatment, that target hepatic cholesterol synthesis by inhibiting 3-hydroxy-3-methylglutaryl-coenzyme A (HMG-CoA) reductase.^{5,13} Statins are the most prescribed drugs but risk causing myopathy, diabetes, weakness through Q10 depletion, etc.¹³ However, these patients have a constellation of pathologies and targeting only one risk factor fails to treat the underlying ill health. Indeed, many of these patients drift into treatment polypharmacy that increases iatrogenic conditions. Traditional medicine with herbal medicines takes a holistic approach to improving overall efficient body function, well-being, and quality of life, a strategy well-suited to metabolic disease. Food derived medicines also provide levels of safety rarely achieved by allopathic drugs.

Mulberries from *Morus alba* L. are a source of nourishment and used as a traditional medicine to relieve fever, hepatic protectant, improve eyesight, and as an antihypertensive.¹⁴ Several pharmacological studies showed that the extracts of this fruit ameliorate diabetes, obesity, hyperlipidemia, and atherosclerosis.^{15–19} Water- or anthocyanin-rich mulberry extracts inhibited LDL oxidation and foam cell formation *in vitro*.¹⁹ Aqueous or etOH extracts of

mulberries improved blood lipids and reduced aortic atherosclerotic lesions and liver lipid accumulation in cholesterol fed rabbits and high-fat fed rats.^{15,17} Thus, mulberries may well be an efficacious treatment in humans, but the predominant use of extracts may not replicate its traditional use by losing pharmacologically active ingredients. Furthermore, extractions are energy-wasteful. However, getting soft fruit, including mulberries, to market before spoilage is challenging, particularly as medicines that need reliable supplies. Freeze-drying mulberries circumvents these problems. Indeed, such preparations also improved lipid profiles.^{20,21}

Nevertheless, data on various mulberry extracts so far described is fragmented and does not account for the diversity of pathologies manifest as metabolic disease. The current study tests how the unrefined product affects some important risk factors and goes some way define some mechanisms involved protecting against vascular disease and fatty liver that could be clinically applied.

2. Material and methods

2.1. Plant sample preparation

Dried mulberry fruit powder (dMF) was obtained from the Thailand Institute of Scientific and Technological Research, Bangkok, Thailand. Ripe mulberries (*M. alba* L.) from Nakhon Pathom province in Thailand were freshly harvested, freeze dried and roller ground to obtain dMF that was stored at -20°C in darkness until use.

2.2. Chemical composition of dMF by LC-MS

dMF was dissolved in water (20 mg/mL), sonicated and 0.22 μm filtered. Separation used a Luna C18(2), 150 \times 4.6 mm, 5 μm column (Phenomenex, USA). The analysis used an Agilent HPLC 1260 consisting of a vacuum degasser, a binary pump, an autosampler and a column thermostat equipped with QTOF 6540 UHD accurate mass (Agilent Technologies, USA). A 20 μL sample (20 mg/mL) was injected into the LC system with a solvent flow rate of 500 $\mu\text{L}/\text{min}$. The mobile phase consisted of a gradient elution between water (solvent A) and acetonitrile (solvent B), both containing 0.1% v/v formic acid. The linear gradient elution was 5–95% for solvent B starting at 0–30 min and post-run for 5 min. The column temperature was controlled at 35 $^{\circ}\text{C}$. The mass analysis was performed using a QTOF 6540 UHD accurate mass spectrometer. The conditions for the dual negative electrospray ionization source were drying gas (N_2) at a flow rate of 10 l/min, a drying gas temperature of 350 $^{\circ}\text{C}$, nebulizer 30 psig, fragmentor 100 V, capillary voltage 3500 V, skimmer, 65 V, octapole (OCT 1 RF Vpp), 750 V and scan spectra from m/z 100–1000 amu. The auto MS/MS for the fragmentation was set with collision energies of 10, 20 and 40 V. The positive mode was also set up with the same MS conditions as the negative mode. The data were processed by the Agilent MassHunter Qualitative Analysis software version B.06.0, which provided a list of possible molecular formulas. The MS data, MS/MS fragmentation profiles and molecular formula proposed by the MassHunter were compared with the literature data and some

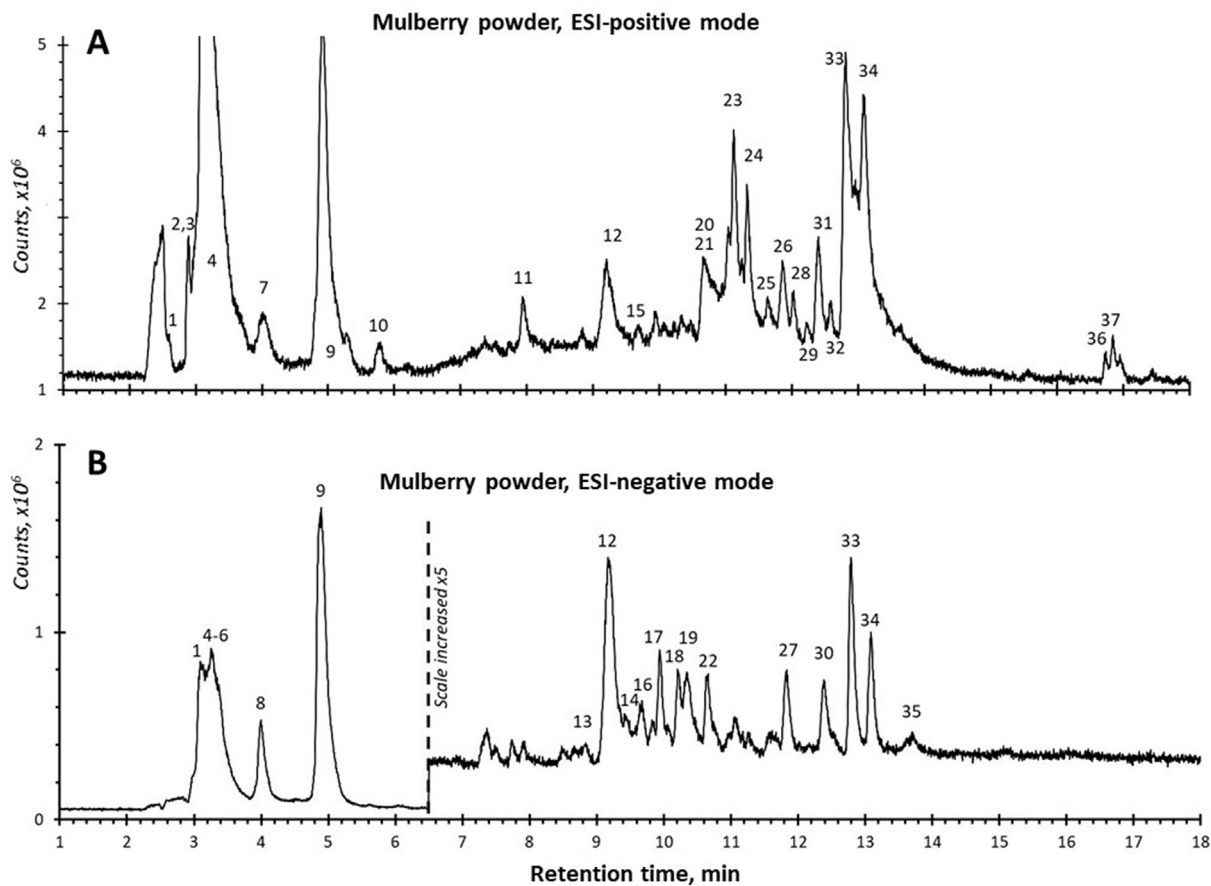


Fig. 1. Total Ion Chromatogram (TIC) of DMF aqueous sample (20 mg/mL) monitored in (A) ESI-positive mode, and (B) ESI-negative mode. The peak numbers correspond to compounds identified in Table 1.

databases, such as Human Metabolome, ChemSpider, METLIN, and Lipidmap to annotate the phytochemicals analyzed from the extracts. The molecular formula proposed by MassHunter in MS experiments was compared with the literature data, and a maximum error of 10 ppm was accepted.

2.3. Anthocyanin content determination and DPPH assay

DMF total anthocyanins were measured by the pH differential method.²² In addition, the reducing ability of the DMF was evaluated by DPPH assay.²³

2.4. Animal and diet

Twenty four female C57BL/6J mice (aged 8 weeks; weight 18–20 g) were obtained from the Nomura Siam International Co. Ltd., Bangkok, Thailand. Experiments were approved by Naresuan University Animal Care and Use Committee (NUACUC, Naresuan University, Phitsanulok, Thailand; ethic protocol number NU-AE 610727) for the care and use of animals for scientific purposes. The mice were acclimatized for 1 week in their polycarbonate cages at 22 ± 1 °C, 12–12 h light–dark cycle, and allowed access to food and water *ad libitum* at the Center for Animal Research, Naresuan University, Phitsanulok, Thailand. The animals were randomly divided into 4 groups each of which were fed a different diet for 3 months;

- i) Control: Animals were fed with normal diet (Teklad Global: “18% Protein Rodent Diet”, 3.1 kcal/g containing 6.5% fat, 44.2% carbohydrate, 18.6% protein from Harlan Teklad Laboratory, Madison, Wisconsin, USA), and gavaged with water.
- ii) High fat diet (HF): Animals were fed with HF (Harlan Teklad Atherogenic Rodent Diet, 4.5 kcal/g composed of 21.2% fat, 0.2% cholesterol, 46.9% carbohydrate, 17.3% protein) and gavaged with water. Since the pellets were more friable than the standard diet, they were treated with polyvinylpyrrolidone to match their hardness and strength of the standard pellets.
- iii) HF+100 mg/kg DMF (HF + dMF100): Animals were fed with HF and dMF was administered by gastric tube once daily as an aqueous suspension.
- iv) HF+300 mg/kg DMF (HF + dMF300) Animals were fed with HF and dMF was administered by gastric tube once daily as an aqueous suspension.

All animals were weighed and food intake was measured daily throughout the 3 month test period. At the end of the experiment, mice were fasted (12–14 h), deeply anesthetized by 50–70 mg/kg sodium thiopental intraperitoneally. Then blood, aorta, heart, liver and visceral fat were removed as below.

2.5. Visceral fat accumulation

Visceral fat was manually separated from the abdominal cavity, then weighed and expressed as g/100 g body weight.

Table 1
MS data of (\pm) ESI- QTOF-MS/MS and the structure elucidation of dMF aqueous sample.

Peak RT (min)	<i>m/z</i>	adduct	Fragmentation (MS/MS)	Tentative Identification	Formula	Error (ppm)
1	3.119	324.1299 [M-H] ⁻	144.0656	2-O- α -D-Galactopyranosyl-1-deoxynojirimycin	C12H23NO9	0.32
	2.613	326.1447 [M+H] ⁺	164.092	2-O- α -D-Galactopyranosyl-1-deoxynojirimycin	C12H23NO9	-0.44
2	2.882	104.1071 [M] ⁺	60.0814	Choline	C5H14NO	4.22
3	2.935	266.1243 [M+H] ⁺	248.1138,230.1035,182.0812,98.0600	D-1-[(3-Carboxypropyl)amino]-1-deoxyfructose	C10H19NO7	-3.28
4	3.173	179.0562 [M-H] ⁻	89.0236,59.0137	Glucose	C6H12O6	-0.49
	3.118	203.0535 [M+Na] ⁺	112.1140,84.0823	Glucose	C6H12O6	-4.39
5	3.306	277.0332 [M-H2O] ⁻	96.9690,78.9586	Caffeoylmalic acid	C13H12O8	7.86
6	3.405	191.0562 [M-H] ⁻	85.0288	Quinic acid	C7H12O6	-0.46
7	3.993	280.1402 [M+H] ⁺	262.1334,244.1219,216.1273,72.0821	N-(1-Deoxy-1-fructosyl)valine	C11H21NO7	-4.0
8	3.999	133.0139 [M-H] ⁻	115.0026,71.0135	Malic acid	C4H6O5	2.61
9	4.896	191.0197 [M-H] ⁻	111.0085,87.0085,57.0345	Citric acid	C6H8O7	2.75
	4.914	215.0173 M + Na] ⁺	193.1245	Citric acid	C6H8O7	-5.01
10	5.771	132.102 [M+H] ⁺	86.0962	Leucine	C6H13NO2	-0.72
11	7.943	166.0868 [M+H] ⁺	120.0803,84.9595	L-Phenylalanine	C9H11NO2	-3.28
12	9.18	611.1591 [M + H2O] ⁻	475.1425,285.0384,241.0488,149.0227,125.0235	Cyanidin 3-rutinoside	C27H31O15	4.35
	9.183	593.1487 [M-H] ⁻	284.0306,125.0231	Cyanidin 3-rutinoside	C27H31O15	4.2
	9.191	595.1671 [M] ⁺	449.1066,287.0544,213.0523	Cyanidin 3-rutinoside	C27H31O15	-1.35
13	9.366	353.0857 [M-H] ⁻	191.0548,179.0353,135.0442	Caffeoylquinic acid	C16H18O9	5.96
14	9.441	771.1941 [M-H] ⁻	609.1396,463.0809,301.0323	Quercetin 3-O-glucosyl-rutinoside	C33H40O21	6.27
15	9.641	579.1693 [M] ⁺	433.1119,271.0589	Pelargonidin 3-rutinoside	C27H31O14	3.59
	9.704	433.1135 [M] ⁺	271.0592	Pelargonidin 3-glucoside	C21H21O10	-0.06
16	9.718	339.0696 [M-H] ⁻	177.0175	p-Coumaric acid glucuronide	C15H16O9	7.54
17	9.947	611.1588 [M + H2O] ⁻	475.1420,285.0386,241.0480,149.0232,125.0234	Cyanidin 3-O-(6''-O- α -rhamnopyranosyl)- β -D-glucopyranoside	C27H31O15	4.84
	9.947	635.159 [M+Na] ⁺	489.0969,331.0972,309.0337,287.0475			-1.17
18	10.1008	465.1008 [M + H2O] ⁻	329.0846,285.0385,241.0479,125.0227	Cyanidin 3-glucoside	C21H21O11	6.56
19	10.363	353.0867 [M-H] ⁻	191.0542,179.0334,135.0442	Caffeoylquinic acid	C16H18O9	3.13
20	10.625	492.3185 [M+H] ⁺	474.3042,330.2628,252.2317,70.0647	Morusimic acid derivative	C24H45NO9	-3.64
21	10.654	563.2117 [M+H] ⁺	401.1551,365.1188	5,7-Dihydroxy-3',4'-dimethoxy-8-(3-hydroxy-3-methylbutyl)-isoflavone 7-glucoside	C28H34O12	1.07
22	10.96	353.0857 [M-H] ⁻	191.0545	Caffeoylquinic acid	C16H18O9	5.96
23	11.125	492.3181 [M+H] ⁺	330.2626,268.2625,250.2519,85.0278	Morusimic acid derivative	C24H45NO9	-2.83
24	11.328	492.3177 [M+H] ⁺	330.2622,268.2624,250.2518	Morusimic acid derivative	C24H45NO9	-2.01
25	11.635	578.316 [M+H] ⁺	534.3233,330.2615,268.2621,250.2517	Morusimic acid derivative	C27H47NO12	1.91
26	11.895	534.3266 [M+H] ⁺	474.3032,372.2722,312.2521,250.2516	Morusimic acid derivative	C26H47NO10	1.26
27	11.818	609.1421 [M-H] ⁻	300.0258	Rutin	C27H30O16	6.58
28	12.019	330.2638 [M+H] ⁺	312.2522,250.2517,70.0645	Morusimic acid derivative	C18H35NO4	0.26
29	12.23	330.2636 [M+H] ⁺	312.2516,250.2519	Morusimic acid derivative	C18H35NO4	0.86
30	12.359	303.0496 [M-H] ⁻	167.0337,165.0167,109.0285	Taxifolin	C15H12O7	4.71
31	12.4	566.4252 [M+H] ⁺	548.4148,435.3319,322.2468,209.1637,114.0909,96.0798	Unidentified		
32	12.591	581.3327 [M+H] ⁺	114.1270,72.0801	Unidentified		
33	12.797	723.4976 [M + HCOO] ⁻	677.4926	Contaminate from Nylon membrane		
	12.804	701.493 M + Na] ⁺				
34	13.092	826.5528 [M+Cl] ⁻	790.5746	Contaminate from Nylon membrane		
		814.506 [M+Na] ⁺				
35	13.72	303.0496 [M-H] ⁻	285.0383,177.0183,125.0232,57.0344	(2e)-1-(2,4,6-trihydroxyphenyl)-3-(3,4,5-trihydroxyphenyl)prop-2-en-1-one	C15H12O7	4.71
36	16.73	274.2752 [M+H] ⁺	256.2637,106.086088,0753,70.0651,57.0697	Hexadecaphinganine	C16H35NO2	-4.17
37	16.841	318.3015 [M+H] ⁺	256.2646,88.0760,70.0653,57.0701	Phytosphingosine	C18H39NO3	-3.86

2.6. Blood lipid profile

Whole blood was collected by cardiac puncture and transferred to heparin-coated tubes, centrifuged at 3000 g, 4 °C for 10 min and the plasma retained. Plasma levels of total cholesterol (TC), triglyceride (TG), and high density lipoprotein (HDL) were measured using an enzymatic colorimetric test according to manufacturer protocols (Human diagnostic company, Wiesbaden, Germany). Plasma LDL was calculated by the following equation: $LDL = TC - (HDL + TG/5)$.

2.7. Blood glucose analysis

Before euthanasia, the tip of tail was cut and ~10 μ L of blood directly dropped on to test strips and blood glucose measured using a ACCU-Chek Performa blood glucose monitor (Roche Diabetes Care, Mannheim, Germany).

2.8. Determination of histological changes in aorta and heart tissue

Aorta and heart were quickly separated, rinsed with normal saline and then cleaned of fat and fixed with buffered 10% formalin, dehydrated, and embedded in paraffin. De-waxed sections of 3–5 μ m were stained by Masson's trichrome for collagen. Sections were photographed via light microscopy and analyzed by Image J (version 1.51j8, National Institutes of Health, USA). Areas of collagen fibre accumulation in the tunica media was calculated as a percentage of the total area of tunica media bounded by the internal elastic lamina and the external elastic lamina.

2.9. Hepatic lipid accumulation

Livers were washed with normal saline and then preserved in 30% sucrose in paraformaldehyde at 4 °C. They were cut at 10 μ m as frozen sections, stained with oil red O, mounted in Permount', and

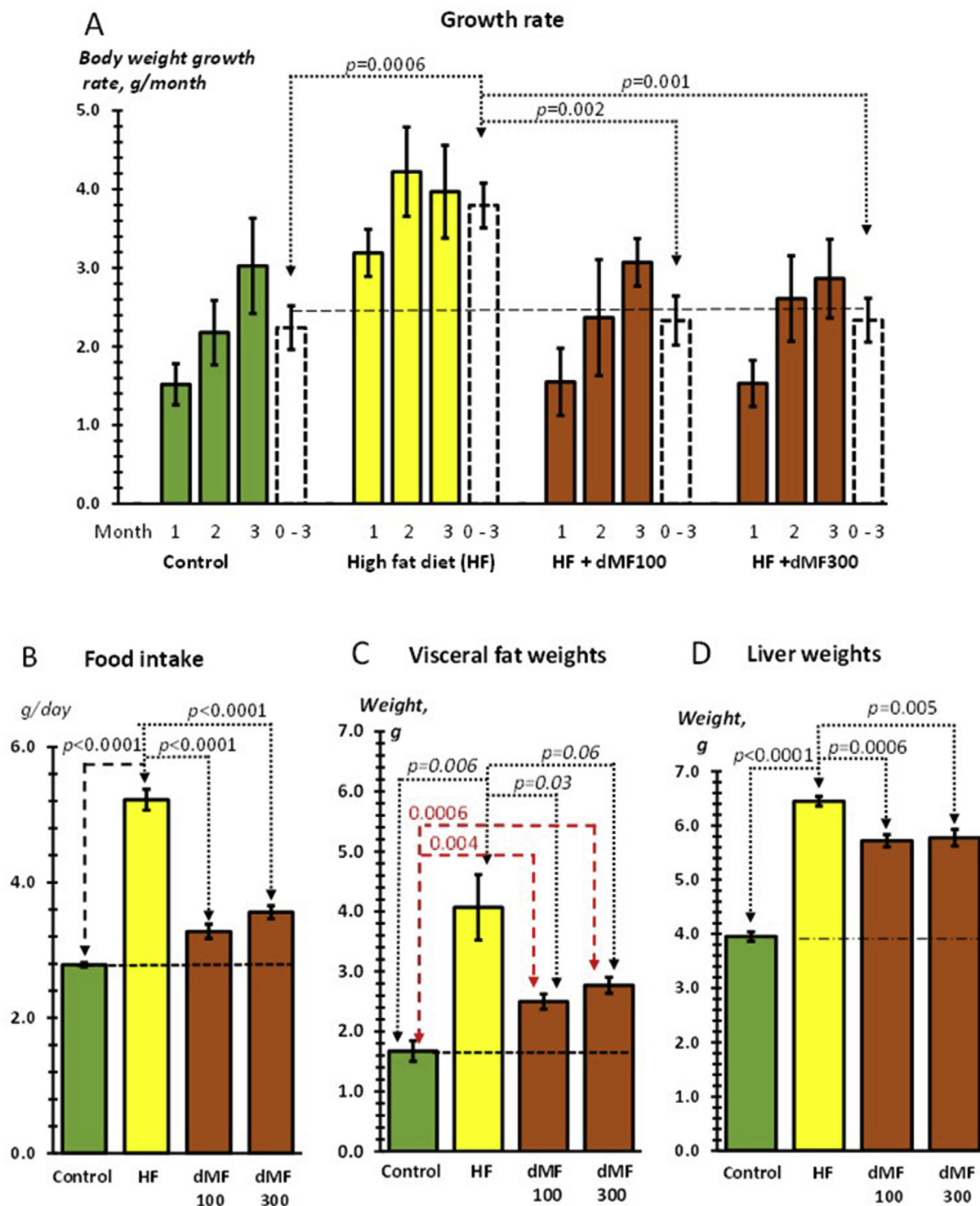


Fig. 2. (A) Growth rates by weight through the 3 month protocol. The white bars are averaged values for the 3 month period for each treatment. Error bars are SEMs and the P-values are for unpaired, 2-tailed comparisons denoted by the dotted lines. (B) Food intake averaged over 12 weeks. n = 7 mice. Data pooled with more values from previous study.⁵³ (C) Weights of visceral fat after 3 months of treatment. Dotted lines compare high fat diet with all other groups. P-values in red compare control with each dMF dose. (D) Liver weights.

photographed at 40× magnification by light microscopy. Images were analyzed by Image J software (version 1.51j8, National Institutes of Health, USA) to quantify liver lipid area occupied by oil red O positive staining and expressed as the proportion of region of interest (%).

2.10. Autophagy immunohistochemistry of liver

Liver samples were collected and fixed in 10% neutral buffered formalin before paraffin embedding (FFPE). For immunohistochemistry (IHC) evaluations, 4 μm sections of FFPE liver tissue were

mounted onto commercially coated glass slides, dried at room temperature, and incubated at 65 °C for 1 h prior to use. Sections were deparaffinized/hydrated. For antigen unmasking, sections were submersed in 1x citrate unmasking solution, heated to boiling point and left for 10 min (at 95°-98 °C) and then cooled for 30 min. Endogenous peroxidases were blocked by incubating with 3% hydrogen peroxide for 10 min. The sections were washed in deionized water and wash buffer, then each section blocked with 100–400 µL of TBST/5% normal goat serum for 1 h at room temperature. After removing the blocking solution, rabbit monoclonal anti-LC3A/B (1:500, Cell Signaling, USA) or rabbit monoclonal anti-SQSTM1/p62 (1:250, Cell Signaling, USA) were added to each section. These were incubated overnight at 4 °C. The sections were washed by wash buffer before covering with IHC detection reagent (UltraView Universal HRP multimer, Ventana, USA) and incubated in a humidified chamber for 30 min at room temperature. Signal-Stain® DAB chromogen was applied on each section. Tissue sections were counterstained with hematoxylin and then dehydrated using 95% ethanol, 100% ethanol, and xylene and mounted in mounting medium. The slides stained for LC3A/B and SQSTM1/p62 were photographed with Olympus microscope using cell Sens Imaging Software. Numbers of hepatocytes positive for LC3 A/B or SQSTM1/p62 were counted using image J.

2.11. dMF on adipocyte function

dMF was tested on pre-adipocyte differentiation (adipogenesis) and fat loss from mature adipocytes (lipolysis). 3T3-L1 pre-adipocytes were cultured in high glucose Dulbecco’s Modified Eagle’s Medium (DMEM) supplemented with 10% fetal bovine serum and 1%/mL penicillin/streptomycin as completed medium under a humidified 5% CO₂ atmosphere at 37 °C in CO₂ incubator. Inhibition of lipid accumulation by dMF was assessed as reported.²⁴ After reaching confluence in flasks, cells (2 × 10³ cells/well) were seeded into 96 well plates and cultured in complete media for 2 days.

Action of dMF on adipocyte differentiation: The medium was changed to adipocyte differentiation medium, complete medium containing with added: dexamethasone (1 µM DEX); isobutylmethylxanthine (0.5 mM, IBMX); and insulin (10 µg/mL), to initiate adipocyte differentiation (defined as day 1), also with dMF (20, 50, 100, 200, 500, or 1000 µg/mL). This medium was removed at days 3, 5 and 7 and replaced with complete medium with 10 µg/mL insulin and dMF only. At day 9, cells were tested for either (i) lipogenesis by cell content using oil red O staining, or (ii) cell viability using 3-(4,5-dimethylthiazol-2-yl)-2,5-diphenyltetrazolium bromide (MTT). Cells without dMF served as negative controls.

Action of dMF on lipolysis: For lipolysis, a similar protocol was used for 9 days but without dMF using adipocyte differentiation medium and supplemented with 10 µg/mL insulin only. At day 9,

dMF (20, 50, 100, 200, 500, or 1000 µg/mL) was then added to the medium and further incubated for 24 h. Finally, treated cells were assessed for either lipid content, or cell viability.²⁴

For assay of adipocyte lipid content²⁵ cells, were washed twice with of PBS (100 µL), fixed with 10% formalin/PBS (100 µL) for 8 min and 1 h, and then washed twice with 100 µL of 60% isopropanol. The cells were allowed to dry in room air. Then 50 µL of 0.5% oil Red O in distilled water was added and incubated for 45 min, then washed twice with 100 µL distilled water. The dye was extracted with 100 µL of isopropanol, shaken for 10 min, and optical density of the solution measured at 500 nm using microplate reader. Lipid contents were expressed as absorbance compared to control (untreated cells = 100%).

For cytotoxicity testing by the MTT assay,²⁶ cells were incubated with MTT reagent (0.5 mg/mL) for 4 h at 37 °C in CO₂ incubator. Then, the solution was discarded and DMSO (100 µL) was added and shaken for 15 min to dissolve formazan crystals. The absorbance was recorded at 595 nm using microplate reader. Cell survival expressed as absorbance compared to control (no treatment = 100%).

2.12. Bile acid binding assay

The bile acid binding to dMF was measured as previously reported.²⁷ dMF was dissolved in distilled water, well mixed and diluted to 0.2, 2, 10, and 20 mg/mL of dMF. dMF solution (200 µL) (final concentrations 0.1, 1, 5, and 10 mg/mL) was incubated with 20 µL of 20 mM bile acids (taurocholic acid or taurodeoxycholic acid) with phosphate buffer saline (PBS) (180 µL) for 2 h at 37 °C. The mixtures were centrifuged at 10,000 rpm for 20 min and filtered through a 0.22 µm filter. The filtrate (10 µL) was reacted with 1 unit of 3α-hydroxysteroid dehydrogenase (10 µL) in 180 µL of reaction mixture (tris buffer pH 9.5; 1 M hydrazine hydrate; 7.7 mM nicotinamide adenine dinucleotide (NAD), ratio of 1.5:1:0.3) at 30 °C. Cholestyramine and PBS were used as positive and negative controls, respectively. After being incubation for 90 min, the optical density of reactions was measured at 340 nm using microplate reader. The percentage of bile acid binding was compared with control (no treatment) which considered as 0%.

2.13. Statistical analysis

All data were expressed as mean ± standard error of mean (SEM) of n animals. The statistical significance between groups was evaluated using student t-test and/or ANOVA followed by the Tukey–Kramer post hoc test. Values of P < 0.05 were considered statistically significant.

Table 2 Plasma lipid profiles and blood glucose level at 3 months.

Parameters	Control	HF	HF + dMF100 mg/kg	HF + dMF 300 mg/kg
Plasma lipid (mg/dL)				
TC	60.9 ± 1.2	127.6 ± 4.6**	118.4 ± 4.5**	116.7 ± 9.4**
TGs	70.5 ± 4.1	70.2 ± 2.7	49.5 ± 3.6**###	46.8 ± 1.9**###
HDL	37.2 ± 2.1	34.9 ± 4.3	44.2 ± 1.0*,##	46.4 ± 0.6**###
LDL	19.4 ± 2.8	71.4 ± 5.0**	64.5 ± 8.1*	64.5 ± 12.0*
TC/HDL	1.6 ± 0.1	3.6 ± 0.2**	2.62 ± 0.1*,##	2.59 ± 0.2*,##
Blood glucose (mg/dL)				
Baseline	95.5 ± 1.6	97.3 ± 5.2	94.8 ± 4.2	97.7 ± 2.9
3 months	94.2 ± 2.5	113.7 ± 3.9**	94.3 ± 0.7###	99.8 ± 3.0#

Control, normal diet; HF, high-fat diet; HF + dMF 100, high fat diet+100 mg/kg dried mulberry fruit powder; HF + dMF 300, high-fat diet+300 mg/kg dried mulberry fruit powder; TC, total cholesterol; TGs, triglycerides; HDL, high density lipoprotein cholesterol; LDL, low density lipoprotein cholesterol. Values are means ± SEM (n = 6). *P < 0.01, **P < 0.001 vs. control. #P < 0.05, ##P < 0.01, ###P < 0.001 vs. high fat diet.

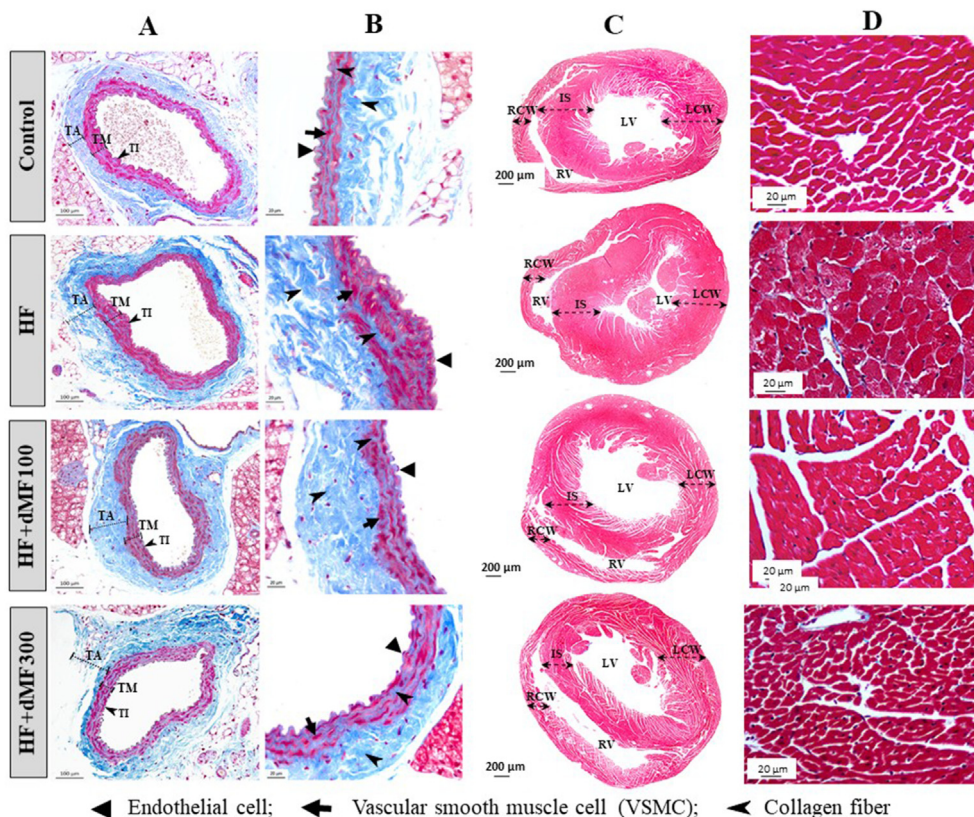


Fig. 3. The histological observation of the aorta and heart stained using Masson's trichrome. Collagen fibers in the tunica media are stained in blue. (A) Aorta at a 10× magnification; (B) Aorta at a 40× magnification, (C) Heart at a 4× magnification, (D) Cardiomyocyte at a 10× magnification. Control, normal diet; HF, high-fat diet; HF + dMF100, high-fat diet +100 mg/kg dried mulberry fruit powder; HF + dMF300, high-fat diet +300 mg/kg dried mulberry fruit powder. TI, Tunica intima; TM, Tunica media; TA, Tunica adventitia; LV, Left ventricle; RV, Right ventricle; LCW, Left cardiac wall; RCW, Right cardiac wall; IS, Interventricular septum.

3. Results

3.1. Composition of dMF

Contents by chemical analysis: Total anthocyanin content by the pH differential method was 1.46 g/100 g dMF.

Contents by LC-MS: Water soluble constituents of dMF yielded 37 peaks corresponding to tentatively identifiable compounds by their monoisotopic mass and fragmentation patterns (Fig. 1; Table 1). Adducts depended on ionization mode: peaks manifest in either mode for some compounds or only seen with either negative or positive mode. Hexoses and organic acids formed a large proportion of the content, while components having possible pharmacological actions formed 4 groups: (i) anthocyanins as cyanidins or pelargonidin glycosides (compounds 12, 15, 17, and 18); (ii) flavonols as rutin (27), and taxifolin (30), (iii) phenolic acids, as conjugates of caffeic acid and quinic acid (5, 6, 16, 19, 22); (iv) Amino acid

compounds and other nitrogen contain compounds (1–3, 7, 10, 11, 20, 23–26, 28, 29, 36, 37).

3.2. Body weight gain, food intake, visceral fat and liver weight

Gains in body weight were consistently greater for mice on the HF diet than controls by ~100% at one month but less so for months 2 and 3 (Fig. 2A). Weight gains for the dMF-dosed groups (both 100 and 300 mg/kg) prevented almost all the weight gain ascribed to the HF at month 1, but less pronounced for the remaining 2 months (Fig. 2A). These weight changes mirrored changes in food intake which was doubled with the HF and likewise reduced by 100 and 300 mg/kg dMF (Fig. 2B).

The HF substantially increased the amount of visceral fat and the liver weight (Fig. 2C and D). Some of the increased visceral fat and liver weight was prevented by both dMF dose regimens, a ~60% reduction for visceral fat and ~30% for liver.

Table 3
Aortic wall thickness and collagen content, and hepatic lipid accumulation.

Parameters	Control	HF	HF + dMF100	HF + dMF300
Aortic wall thickness (μm)	275 ± 8	386 ± 11*	314 ± 6*,##	338 ± 6*,##
Area of medial collagen (%)	31.5 ± 1.3	48.9 ± 1.2*	39.5 ± 1.6*,##	40.9 ± 1.4*,##
Proportion of hepatic lipid (%)	33.6 ± 2.1	51.9 ± 1.2**	43.0 ± 2.6*, #	42.0 ± 1.6*, #

Control, normal diet; HF, high-fat diet; HF + dMF100, high-fat diet+100 mg/kg dried mulberry fruit powder; HF + dMF300, high-fat diet+300 mg/kg dried mulberry fruit powder. Aortic wall thickness was measured as the perpendicular distance between the inner wall of the tunica intima to the outer extremity of the tunica media. Hepatic lipid was the area occupied by oil red O positive staining and expressed as the proportion of region of interest area. Values are means ± SEM (n = 5 mice). *P < 0.01, **P < 0.001 vs. Control. #P < 0.05, ##P < 0.01 vs. HF.

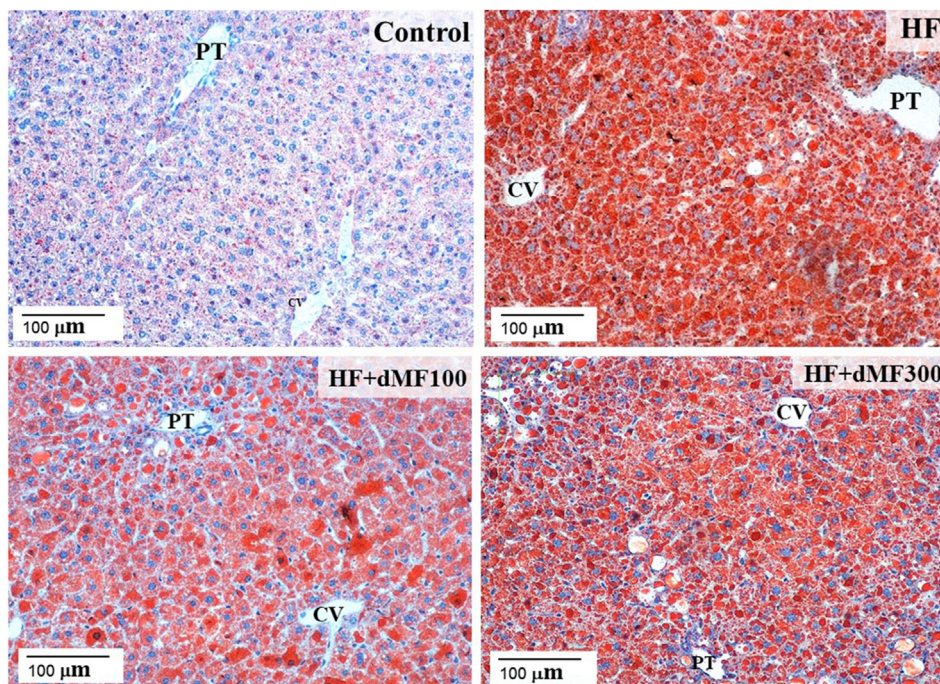


Fig. 4. Oil-Red-O partition into hepatic fat droplets in frozen sections of livers from mice fed diets as indicated. CV, central vein; PT, portal triad; HF, high-fat diet; dMF, dried mulberry fruit powder.

3.3. Plasma lipids and glucose

Three months on the HF raised plasma TC, LDL cholesterol, and glucose as commonly seen with such nutrition (Table 2). TGs and HDL cholesterol were unchanged. In dMF treated mice, TC and LDL cholesterol were not substantially affected but TGs were substantially reduced even below the control while glucose matched the control concentration. HDL was raised even above the control level with dMF (Table 2).

3.4. Changes to aortic and cardiac histology

The major morbidities of metabolic syndrome arise from vascular insufficiencies including arterial stiffening and cardiac hypertrophy. Thus, the aortic wall became hypertrophied (Fig. 3A and B, Table 3) due in part to increased medial collagen due to increased dietary fat. Treatment with either 100 or 300 mg/kg dMF prevented around 50% of aortic wall-thickening ascribed to collagen accumulation (Fig. 3A and B, Table 3).

The HF also produced a hypertrophy of the left ventricular wall (Fig. 3C) and expansion of constituent cardiomyocyte (Fig. 3D). More collagen deposition was as well observed, in particular around the blood vessels of the heart in the HF group (Fig. 3C and D), but this was less pronounced in the dMF-treated groups (Fig. 3D).

3.5. Liver lipid accumulation

Hepatic lipid content was measured directly using ‘oil red O’ that showed sparse staining in the control group, intense in the HF group, and substantial in the dMF-fed groups (Fig. 4). The incremented oil red O contents in the HF group was lowered by 49% in the two dMF groups as summarised in Table 3.

3.6. Autophagy by LC3 and p62 immunohistochemistry

The next experiments aimed to assess the role of autophagy in fatty liver disease by measuring expression of two marker proteins, LC3 (Fig. 5) and p62 (Fig. 6), involved in recycling dysfunctional proteins. The IHC using anti-LC3 antibody showed 4 types of distinct staining patterns of hepatocytes: no staining (0), feint (1+), intermediate (2+), and strong staining (3+). Endothelial and Kupffer cells lining the sinusoids stained intensely (Fig. 5). For a positive control, cerebral neurons also stained (Fig. 5E).

Cells identified as hepatocyte were counted according to staining category (Fig. 5) in 7 photomicrographs taken at random from livers of each of 4 mice. From all of 16 mice used, the average hepatocyte count was 2490 ± 386 (SD) of which 88 ± 56 were graded 1+, 44 ± 36 , 2+, and 14 ± 14 3+ across all 112 frames. Stained hepatocytes tended to exist in groups which explained their highly variable count rates. Fig. 5F shows the proportions of all staining categories counted hepatocytes. Fig. 5E shows an IHC positive control using neocortex processed at the same time.

The ubiquitin-binding protein p62 is also involved in hepatic autophagy. The p62 positive cells tended to be confined to regions, and their numbers tended to increase in dMF treated group (Fig. 6E). There is no clear evidence that liver autophagy was dramatically changed for either marker protein.

3.7. Lipid accumulation and lipolysis in adipocytes

3T3-L1 cells were cultured in media that stimulated proliferation and promoted fat accumulation and inhibition of these processes could reduce cell fat content. dMF marginally reduced lipogenesis (Fig. 7A) while the cell viability was unaffected (Fig. 7B). Fat mass can also be lowered by mobilising accumulated TG stores through lipolysis to fatty acids and glycerol that are then metabolised or lost to the medium. Treatment of cells with the lipolysis protocol for just 24 h reduced fat content with the higher dMF concentrations (Fig. 7C) without adversely affected cell viability

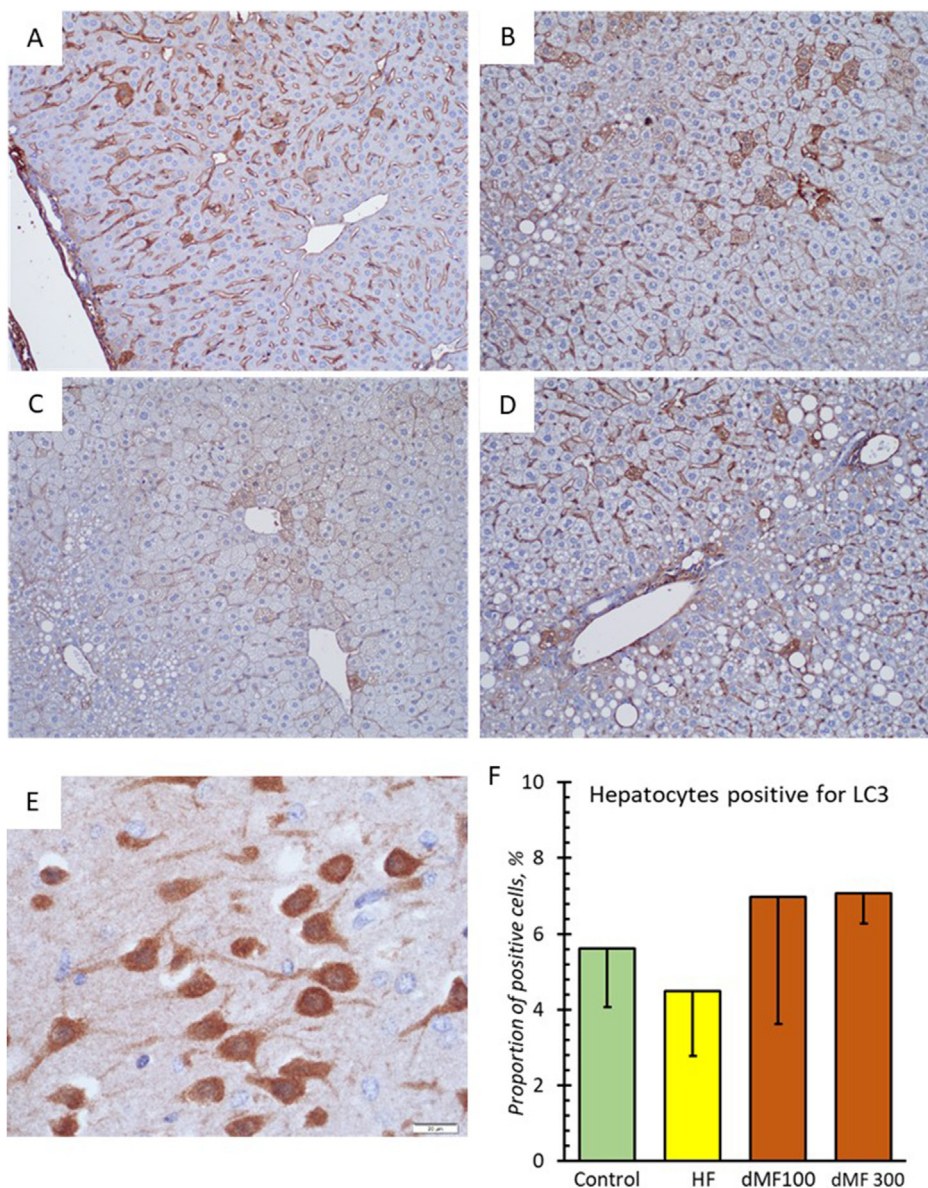


Fig. 5. Representative photomicrographs of immunohistochemical staining for LC3 in control group (A), HF group (B), HF + dMF100 (C), HF + dMF300 (D), neocortical neurons showing somatic and dendritic staining as a positive control (E) and proportion of positive cells (F). Proportion of LC3 positive cells was not different between groups. Values are mean \pm SEM (n = 4). Control, normal diet; HF, high-fat diet; HF + dMF 100, high-fat diet +100 mg/kg dried mulberry fruit powder; HF + dMF 300, high-fat diet +300 mg/kg dried mulberry fruit powder.

(Fig. 7D).

3.8. Bile acid binding activity of dMF

Sequestration of bile acids is used clinically to prevent intestinal fat absorption. While cholestyramine bound strongly to taurocholic acid and taurodeoxycholic acid, binding of dMF to these bile acids was generally undetectable except for very weak binding at 1 g/mL (Table 4) and thus unlikely to influence fat absorption.

4. Discussion

Increased dietary fat fed to mice induced many of the cardiovascular, biochemical risk factors, and histological changes associated with metabolic disease seen in humans. Specifically, HF consumption accelerated body weight gain, promoted visceral and

hepatic fat accumulation, changes that were prevented or reduced by concomitant administration of 100 and 300 mg/kg dMF. HF increased fasting blood glucose, plasma TC, LDL and the TC/HDL ratio. Both dMF doses normalised blood glucose, reduced TC/HDL, and remarkably reduced TGs below the control level while elevating HDL above baseline level. The latter suggests that dMF might have benefits in the absence of an atherogenic diet. In contrast, dMF had little impact on TC and LDL. These observations generally reflect mouse studies using statins and mulberry extracts that reduce obesity,^{28–33} diabetes^{34–38} and hyperlipidemia^{21,30,39}

The hyperglycemia and dyslipidemia in HF mice was accompanied by deterioration in cardiovascular histology, i.e., fibrosis of the aortic wall that diminishes vascular compliance. With accompanying endothelial inflammation, the endothelial vasodilatory signalling is reduced leading to poorer tissue perfusion and feedback compensation that increases cardiac output and arterial

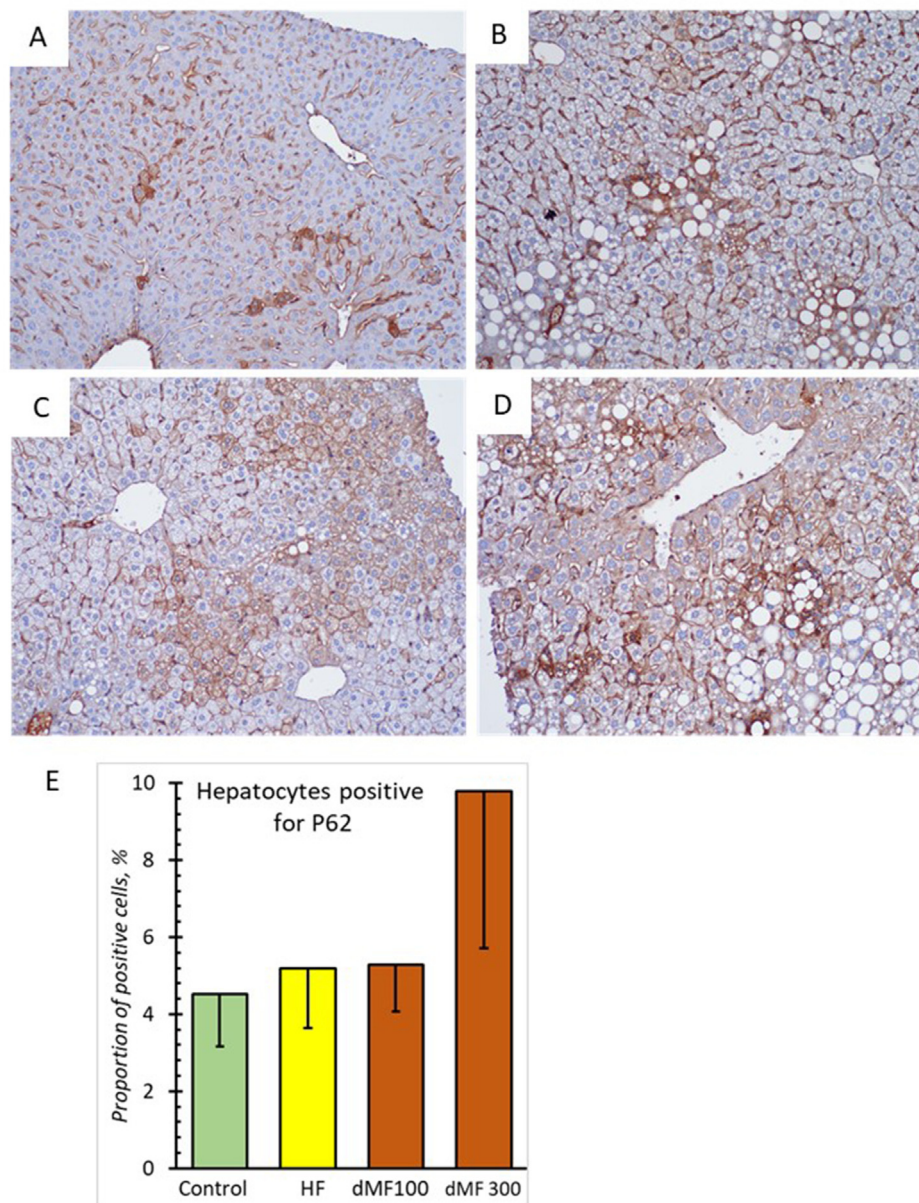


Fig. 6. Representative photomicrographs of immunohistochemical staining for p62 in brown for the control group (A), HF group (B), HF + dMF 100 (C), and HF + dMF 300 (D). Proportion of p62 positive cells was not different between groups (E). Values are mean \pm SEM (n = 4). Control, normal diet; HF, high-fat diet; HF + dMF100, high-fat diet +100 mg/kg dried mulberry fruit powder; HF + dMF300, high-fat diet +300 mg/kg dried mulberry fruit powder.

hypertension to maintain tissue perfusion. This sustained cardiac demand drives left ventricular myocyte hypertrophy that was clearly observed in our study. These observations accord characteristics of atherosclerosis.^{7,8}

dMF Mechanisms of action: Inflammation underlies metabolic disease and all its cardiovascular ramifications. Anthocyanins are widely known for their beneficial cardiovascular supported by numerous investigations and convincing clinical trials.⁴⁰ Of the dMF constituents, some polyphenols and especially the total cyanidin oral dose (as 3-glycosides) was \sim 1.5 mg/kg in 100 mg dMF. Bioavailabilities are low with oral anthocyanin doses higher than administered here, typically achieving blood concentrations of <1 μ M and slightly higher for aglycone.⁴¹ Cyanidin conjugates are readily hydrolysed by enterocytes and numerous intestinal bacterial species.⁴² The gut microbiome also cleave the 'C' ring to yield two monocyclic polyphenols that are more bioavailable than

cyanidins and achieve effective blood concentrations in humans.⁴³ These metabolites have widespread anti-inflammatory effects, especially on vascular endothelial cells, some acting \sim 100 nM.⁴⁴ Microbial metabolism of other polyphenols also generate the same monocyclic metabolites augmenting those from cyanidins.⁴⁵ Polysaccharides may also contribute to dMF actions⁴⁶ and α -glucosidase inhibition by its galactopyranosyl-1-deoxynojirimycin would help to reduce damaging hyperglycemic peaks in humans. Pharmacologies of other constituents await exploration.

The autophagy marker proteins LC3 and p62 were not convincingly affected by the HF diet nor by dMF as seen in other study.⁴⁷ A related process, lipophagy may be more relevant to cells engorged with fat and provide a way of fat mobilisation.

The doubling of HF food intake and commensurate weight gain is common yet overlooked by many studies but the cause of such hyperphagia is unclear.⁴⁸ dMF prevented the hyperphagia

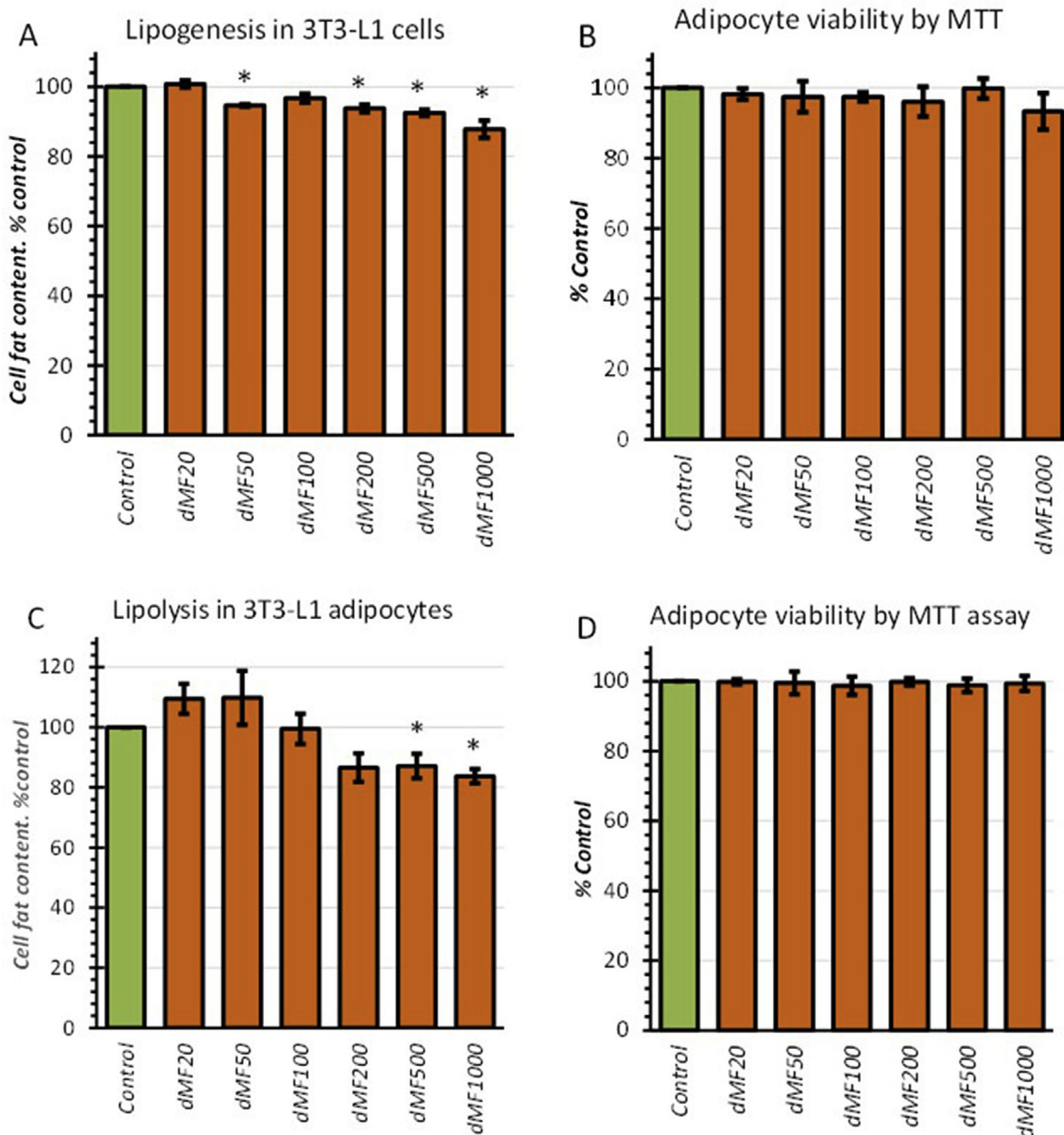


Fig. 7. Effect of dried mulberry fruit (dMF, 20–1000 µg/mL) in cultured 3T3-L1 adipocytes on (A) Lipogenesis (lipid accumulation) measured by oil red O staining; (B) Cell viability using the MTT assay; (C) Lipid loss by lipolysis; and (D) Cell viability using the MTT assay. Values are means ± SEM (n = 3), *P < 0.05 vs. Control.

Table 4
Binding of dMF or cholestyramine to bile acids (taurocholic acid and taurodeoxycholic acid) *in vitro*.

Concentrations of dMF or cholestyramine (mg/mL)	Bile acid binding			
	Taurocholic acid		Taurodeoxycholic acid	
	dMF (% of control)	Cholestyramine (% of control)	dMF (% of control)	Cholestyramine (% of control)
0	0.0 ± 0.0	0.0 ± 0.0	0.0 ± 0.0	0.0 ± 0.0
0.1	0.0 ± 0.0	4.9 ± 11.3	0.0 ± 0.0	8.2 ± 13.8
1	0.0 ± 0.0	47.2 ± 3.0**	0.0 ± 0.0	87.3 ± 3.7*
5	0.0 ± 0.0	83.6 ± 2.1**	0.0 ± 0.0	93.8 ± 2.1**
10	16.6 ± 5.9##	87.7 ± 1.7**	10.2 ± 25.5#	96.5 ± 2.6**

dMF, dried mulberry fruit powder. Values are means ± SEM (n = 3).

*P < 0.01, **P < 0.001 vs. control. #P < 0.01, ##P < 0.001 vs. cholestyramine at the same concentration.

accompanied by a reduced dietary fat load. This makes it difficult to unravel dMF actions that arise solely due to reduced fat load associated with the lower food intake from direct actions on

cellular targets.

Clinical applications: Thus, compared to the single target allopathic medicines, dMF potentially acts on a range of

pathologies typical of metabolic disease. At 100 mg/kg/day allometrically translates to 1g of dMF for humans, a palatable and easily consumed supplement. The safety of mulberries, being a commonly consumed fruit, will always out-perform statin safety.⁴⁹ Trials and medical advice focus on weight loss but instead need a multi-pronged approach beginning with dMF supplements and a profound change of diet. The former reduces inflammation and its polyphenols assist microbial diversity,⁵⁰ while the new diet shifts microbial metabolism away from energy harvesting seen in obesity to short-chain fatty acid production that improves enterocyte, immune, and hepatic function.⁵¹ Because metabolic syndrome manifests as a constellation of interacting pathologies, treatment should be holistic as practiced by traditional healers rather than a monotherapy using a single treatment outcome.

Study limitations: Rodents are poor models for human metabolic disease.⁵² Commercial animal diets are formulated to optimise health while human diets are designed to satisfy gustatory drive causing calorie intake in excess of needs, which may create nutrient deficiencies, and create intestinal dysbiosis. Here, we show that mulberries prevent obesogenic pathologies, but treatments for established obesity in human fat mobilisation no longer operate because of adipocyte inflammation, and leptin- and sex hormone-resistance. Nevertheless, researchers have tight control their animal protocols.

Future studies: Human metabolic disease is best studied in human trials where the disease is already entrenched. While tight control of the numerous lifestyle variables is impossible, strict and detailed participant selection criteria greatly facilitates data interpretation. Studies on dMF or any other herbal should be in the context of a holistic treatment and include a quality of life outcome: The trial should aim to: (i) reduce the excess energy input while improving nutrition, and (ii) removing existing adipocyte or ectopic fat through muscular utilisation or mitochondrial thermogenesis. TOF/LC/MS measurement of circulating and fecal metabolites is crucial for defining the actual agents generating the pharmacological efficacy.

5. Conclusion

This study suggests that the lyophilised mulberries can ameliorate dyslipidemia, improve vascular and cardiac function and promote weight loss in mice and the results suggest translation to patients with metabolic syndrome. Animal models may be best used to characterise mechanisms discovered in the human condition. Contemporary application of traditional medicines should study the whole herbal product and its pharmacologically active metabolism in clinical trials. However, to have a major impact on the constellation of disease processes encompassing metabolic syndrome, requires a paradigm shift in lifestyle where dMF serves as an important supplement in the required holistic treatments.

Funding

This work was funded by National research council of Thailand (Grant number: RA2562B087) and Agricultural research development agency (Public organization) of Thailand (Grant number: CRP6205031380).

Declaration of competing interest

The authors declare that there are no conflicts of interest.

Acknowledgments

We would like to thank the Center of Excellence for Innovation

in Chemistry (PERCH-CIC), Thailand and the International Research Network (IRN61W0005), Thailand on research facility support. We are grateful to Dr. C. Norman Scholfield for his constructive criticism of the manuscript.

References

- Clifton PM. Diet, exercise and weight loss and dyslipidaemia. *Pathology*. 2019;51(2):222–226.
- Zhu Z, Wu F, Lu Y, et al. The association of dietary cholesterol and fatty acids with dyslipidemia in Chinese metropolitan men and women. *Nutrients*. 2018;10(8):961.
- Noureddin M, Mato JM, Lu SC. Nonalcoholic fatty liver disease: update on pathogenesis, diagnosis, treatment and the role of S-adenosylmethionine. *Exp Biol Med*. 2015;240(6):809–820.
- Sweet PH, Khoo T, Nguyen S. Nonalcoholic fatty liver disease. *Prim Care*. 2017;44(4):599–607.
- Tomic D, Kemp W, Stuart KR. Nonalcoholic fatty liver disease: current concepts, epidemiology and management strategies. *Eur J Gastroenterol Hepatol*. 2018;30(10):1103–1115.
- Lacy M, Atzler D, Liu R, de Winther M, Weber C, Lutgens E. Interactions between dyslipidemia and the immune system and their relevance as putative therapeutic targets in atherosclerosis. *Pharmacol Ther*. 2019;193:50–62.
- Libby P, Buring JE, Badimon L, et al. Atherosclerosis. *Nat Rev Dis Primer*. 2019;56, 2019.
- Nguyen MT, Fernando S, Schwarz N, Tan J, Bursill CA, Psaltis PJ. Inflammation as a therapeutic target in atherosclerosis. *J Clin Med*. 2019;8(8):1109.
- Hariri N, Thibault L. High-fat diet-induced obesity in animal models. *Nutr Res Rev*. 2010;23:270–299.
- Moulis M, Vindis C. Autophagy in metabolic age-related human disease. *Cells*. 2018;24(10):149, 7.
- Shin DW. Lipophagy: molecular mechanisms and implications in metabolic disorders. *Mol Cell*. 2020;43(8):686–693.
- Ro SH, Jang Y, Bae J, Kim IM, Schaecher C, Shomo ZD. Autophagy in adipocyte browning: emerging drug target for intervention in obesity. *Front Physiol*. 2019;10:22.
- Ward NC, Watts GF, Eckel RH. Statin toxicity: mechanistic insights and clinical implications. *Circ Res*. 2019;124(2):328–350.
- Yuan Q, Zhao L. The Mulberry (*Morus alba* L.) Fruit- A Review of characteristic components and health benefits. *J Agric Food Chem*. 2017;65:10383–10394.
- Chen CH, Liu LK, Hsu JD, Huang HP, Yang MY, Wang CJ. Mulberry extract inhibits the development of atherosclerosis in cholesterol-fed rabbits. *Food Chem*. 2005;91(4):601–607.
- Jiang Y, Dai M, Nie WJ, Yang XR, Zeng XC. Effects of the ethanol extract of black mulberry (*Morus nigra* L.) fruit on experimental atherosclerosis in rats. *J Ethnopharmacol*. 2017;200:228–235.
- Yang DK, Jo DG. Mulberry fruit extract ameliorates nonalcoholic fatty liver disease (NAFLD) through inhibition of mitochondrial oxidative stress in rats. *Evid Based Complement Alternat Med*. 2018;2018:8165716.
- Zhang H, Ma ZF, Luo X, Li X. Effects of mulberry fruit (*Morus alba* L.) consumption on health outcomes: a mini-review. *Antioxidants*. 2018;7(5):69.
- Liu LK, Lee HJ, Shih YW, Chyau CC, Wang CJ. Mulberry anthocyanin extracts inhibit LDL oxidation and macrophage-derived foam cell formation induced by oxidative LDL. *J Food Sci*. 2008;73(6):H113–H121.
- Mahmoud MY. Natural antioxidants effect of mulberry fruits (*Morus nigra* and *Morus alba* L.) on lipids profile and oxidative stress in hypercholesterolemic rats. *Pakistan J Nutr*. 2013;12(7):665–672.
- Yang X, Yang L, Zheng H. Hypolipidemic and antioxidant effects of mulberry (*Morus alba* L.) fruit in hyperlipidaemia rats. *Food Chem Toxicol*. 2010;48:2374–2379.
- Chaovanakikit A, Wrolstad RE. Total anthocyanins and total phenolics of fresh and processed cherries and their antioxidant properties. *J Food Sci*. 2004;69(1):FCT67–FCT72.
- Moore J, Yu L. Chapter 9 Methods for antioxidant capacity estimation of wheat and wheat-based food products. In: Yu I, ed. *Wheat Antioxidants*. United State. John Wiley & Sons, Ltd; 2007:118–172.
- Saraphanchotiwitthaya A, Sripalakit P. Inhibition of lipid accumulation in 3T3-L1 adipocytes by *morinda citrifolia* linn. leaf extracts and commercial herbal formulas for weight control. *Int J Pharm Pharmaceut Sci*. 2016;8(12):199–204.
- Wu M, Liu D, Zeng R, et al. Epigallocatechin-3-gallate inhibits adipogenesis through down-regulation of PPAR γ and FAS expression mediated by PI3K-AKT signaling in 3T3-L1 cells. *Eur J Pharmacol*. 2017;795:134–142.
- Wisutthathum S, Kamkaew N, Inchan A, et al. Extract of *Aquilaria crassna* leaves and mangiferin are vasodilators while showing no cytotoxicity. *J Tradit Complement Med*. 2013:360–365.
- Trisat K, Wonh-on M, Lapphanichayakool P, Tiyaboonchai W, Limpeanchop N. Vegetable juices and fibers reduce lipid digestion or absorption by inhibiting pancreatic lipase, cholesterol solubility and bile acid binding. *Int J Veg Sci*. 2017;23(3):260–269.
- Wu T, Qi X, Liu Y, et al. Dietary supplementation with purified mulberry (*Morus australis* Poir) anthocyanins suppresses body weight gain in high-fat diet fed C57BL/6 mice. *Food Chem*. 2013;141(1):482–487.
- Wu T, Tang Q, Gao Z, et al. Blueberry and mulberry juice prevent obesity

- development in C57BL/6 mice. *PLoS One*. 2013;8(10), e77585.
30. Lim HH, Yang SJ, Kim Y, Lee M, Lim Y. Combined treatment of mulberry leaf and fruit extract ameliorates obesity-related inflammation and oxidative stress in high fat diet-induced obese mice. *J Med Food*. 2013;16(8):673–680.
 31. Choi JW, Synytaya A, Capek P, Bleha R, Pohl R, Park YI. Structural analysis and anti-obesity effect of a pectic polysaccharide isolated from Korean mulberry fruit Oddi (*Morus alba* L.). *Carbohydr Polym*. 2016;146:187–196.
 32. Azzini E, Giacometti, Russo GL. Antiobesity effects of anthocyanins in preclinical and clinical studies. *Oxid Med Cell Longev*. 2017;2017:2740364.
 33. Lee MS, Kim Y. Mulberry fruit extract ameliorates adipogenesis via increasing AMPK activity and downregulating microRNA-21/143 in 3T3-L1 adipocytes. *J Med Food*. 2020;23(3):266–272.
 34. Wang Y, Xiang L, Wang C, Tang C, He X. Antidiabetic and antioxidant effects and phytochemicals of mulberry fruit (*Morus alba* L.) polyphenol enhanced extract. *PLoS One*. 2013;8(7), e71144.
 35. Daveri E, Cremonini E, Mastaloudis A, et al. Cyanidin and delphinidin modulate inflammation and altered redox signaling improving insulin resistance in high fat-fed mice. *Redox Biol*. 2018;18:16–24.
 36. Sarikaphuti A, Nararatwanchai T, Hashiguchi T, et al. Preventive effects of *Morus alba* L. anthocyanins on diabetes in Zucker diabetic fatty rats. *Exp Ther Med*. 2013;6(3):689–695.
 37. Jiao Y, Wang X, Jiang X, Kong F, Wang S, Yan C. Antidiabetic effects of *Morus alba* fruit polysaccharides on high-fat diet and streptozotocin-induced type 2 diabetes in rats. *J Ethnopharmacol*. 2017;199:119–127.
 38. (42) Min AY, Yoo JM, Sok DE, Kim MR. Mulberry fruit prevents diabetes and diabetic dementia by regulation of blood glucose through upregulation of antioxidative activities and CREB/BDNF pathway in alloxan-induced diabetic mice. *Oxid Med Cell Longev*. 2020;2020:1298691.
 39. (43) Lee S, Lee SM, Chang E, Lee Y, Lee J, Kim J. Mulberry Fruit extract promotes serum HDL-cholesterol levels and suppresses hepatic microRNA-33 expression in rats fed high cholesterol/choleic acid diet. *Nutrients*. 2012;12(5):1499.
 40. Kopeć A, Zawistowski J, Kitts DD. Benefits of anthocyanin-rich black rice fraction and wood sterols to control plasma and tissue lipid concentrations in wistar kyoto rats fed an atherogenic diet. *Molecules*. 2020;25(22):5363.
 41. Speciale A, Cimino F, Saija A, Canali R, Virgili F. Bioavailability and molecular activities of anthocyanins as modulators of endothelial function. *Genes Nutr*. 2014;9(4):404.
 42. Eker ME, Aaby K, Budic-Leto L, et al. A review of factors affecting anthocyanin bioavailability: possible implications for the inter-individual variability. *Foods*. 2020;9(1):2.
 43. Warner EF, Smith MJ, Zhang Q, et al. Signatures of anthocyanin metabolites identified in humans inhibit biomarkers of vascular inflammation in human endothelial cells. *Mol Nutr Food Res*. 2017;61(9):170053.
 44. Amin HP, Czank C, Raheem S, et al. Anthocyanins and their physiologically relevant metabolites alter the expression of IL-6 and VCAM-1 in CD40L and oxidized LDL challenged vascular endothelial cells. *Mol Nutr Food Res*. 2015;59(6):1095–1106.
 45. Tan J, Li Y, Hou DX, Wu S. The effects and mechanisms of cyanidin-3-glucoside and its phenolic metabolites in maintaining intestinal integrity. *Antioxidants*. 2019;8(10):479.
 46. Chen C, You LJ, Abbasi AM, et al. Characterization of polysaccharide fractions in mulberry fruit and assessment of their antioxidant and hypoglycemic activities in vitro. *Food Funct*. 2016;7:530–539. <https://doi.org/10.1039/c5fo01114k>.
 47. Parafati M, Lascala A, Morittu VM, et al. Bergamot polyphenol fraction prevents nonalcoholic fatty liver disease via stimulation of lipophagy in cafeteria diet-induced rat model of metabolic syndrome. *J Nutr Biochem*. 2015;26(9):938–948.
 48. Licholai JA, Nguyen KP, Fobbs WC, Schuster CJ, Ali MA, Kravitz AV. Why Do mice overeat high-fat diets? how high-fat diet alters the regulation of daily caloric intake in mice. *Obesity*. 2018;26(6):1026–1033.
 49. Ward NC, Watts GF, Ecker RH. Statin toxicity. *Circ Res*. 2019;124:328–350.
 50. Larrosa M, Luceri C, Vivoli E, et al. Polyphenol metabolites from colonic microbiota exert anti-inflammatory activity on different inflammation models. *Mol Nutr Food Res*. 2009;53(8):1044–1054.
 51. Chambers ES, Preston T, Frost G, Morrison DJ. Role of gut microbiota-generated short-chain fatty acids in metabolic and cardiovascular health. *Curr Nutr Rep*. 2018;7(4):198–206.
 52. Getz GS, Reardon CA. Diet, microbes, and murine atherosclerosis. *Arterioscler Thromb Vasc Biol*. 2018;38(10):2269–2271.
 53. Chatturong U, Chaiwong S, Deetud W, et al. Anti-obesity of dried mulberry fruit powder in mice fed with high-fat diet. *NUJST*. 2021;29(1):1–20.